# Discrete adjoint approximations with shocks

M.B. Giles[1]

Oxford University Computing Laboratory, Oxford, U.K. *giles@comlab.ox.ac.uk*

## 1 Introduction

In recent years there has been considerable research into the use of adjoint flow equations for design optimisation (e.g. [Jam95]) and error analysis (e.g. [PG00, BR01]). In almost every case, the adjoint equations have been formulated under the assumption that the original nonlinear flow solution is smooth. Since most applications have been for incompressible or subsonic flow, this has been valid, however there is now increasing use of such techniques in transonic design applications for which there are shocks. It is therefore of interest to investigate the formulation and discretisation of adjoint equations when in the presence of shocks.

The reason that shocks present a problem is that the adjoint equations are defined to be adjoint to the equations obtained by linearising the original nonlinear flow equations. Therefore, this raises the whole issue of linearised perturbations to the shock. The validity of linearised shock capturing for harmonically oscillating shocks in flutter analysis was investigated by Lindquist and Giles [LG94] who showed that the shock capturing produces the correct prediction of integral quantities such as unsteady lift and moment provided the shock is smeared over a number of grid points. As a result, linearised shock capturing is now the standard method of turbomachinery aeroelastic analysis [HCL94], benefitting from the computational advantages of the linearised approach, without the many drawbacks of shock fitting.

There has been very little prior research into adjoint equations for flows with shocks. Giles and Pierce [GP01] have shown that the analytic derivation of the adjoint equations for the steady quasi-one-dimensional Euler equations requires the specification of an internal adjoint boundary condition at the shock. However, the numerical evidence [GP98] is that the correct adjoint solution is obtained using either the "fully discrete" approach (in which one linearises the discrete equations and uses the transpose) or the "continuous" approach (in which one discretises the analytic adjoint equations). It is not clear though that this will remain true in two dimensions, for which there is a similar adjoint boundary condition along a shock.

In this paper, we consider unsteady one-dimensional hyperbolic equations with a convex scalar flux, and in particular obtain numerical results for Burgers equation. Tadmor [Tad91] developed a Lip' topology for the formulation of adjoint equations for this problem, with application to linear post-processing functionals. Building on this and the work of Bouchut

and James [BJ98], Ulbrich has very recently introduced the concept of shift-differentiability [Ulb02a, Ulb02b] to handle nonlinear functionals of the type considered in this paper. This supplies the analytic adjoint solution against which the numerical solutions in this paper will be compared. An alternative derivation of this analytic solution is presented in an expanded version of this paper [Gil02].

## 2 Analytic adjoint solution

Let $u(x,t)$ be the solution of the scalar equation

$$\frac{\partial u}{\partial t} + \frac{\partial f(u)}{\partial x} = 0, \qquad 0<x<1, \quad 0<t<T$$

subject to initial conditions $u(x,0) = u_0(x)$. Numerical results will be presented later for the Burgers equation for which $f(u) \equiv \frac{1}{2}u^2$, but here we consider a general convex function $f(u)$. If the solution $u(x,t)$ is differentiable, then $u(x,t)$ is constant along straight characteristics defined by $\mathrm{d}x/\mathrm{d}t = \mathrm{d}f/\mathrm{d}u$. We will assume that $\mathrm{d}f/\mathrm{d}u>0$ at $x=0$ and $\mathrm{d}f/\mathrm{d}u<0$ at $x=1$, and therefore the value of $u(x,t)$ is specified on the two side boundaries.

When one is interested in the output functional

$$J(u) = \int_0^1 G(u(x,T))\ \mathrm{d}x,$$

the corresponding adjoint solution satisfies the equation

$$\frac{\partial v}{\partial t} + \frac{\mathrm{d}f}{\mathrm{d}u}\ \frac{\partial v}{\partial x} = 0, \tag{1}$$

subject to the final condition $v = \mathrm{d}G/\mathrm{d}u$ on $t = T$. The linearised functional corresponding to a linearised source term $s(x,t)$ can then be expressed as

$$\tilde{J} = \int\!\!\int_\Omega vs\ \mathrm{d}x\,\mathrm{d}t, \tag{2}$$

which can be evaluated without computing the linearised solution to the original equation. This is the basis of the use of adjoint solutions in both design optimisation and error analysis for specific output functionals.

When there is a shock, as illustrated in Figure 1, the adjoint equation remains valid on either side of the shock, but along the shock the adjoint solution has value $([G]/[u])_{t=T}$, the ratio of the jumps in $G(u)$ and $u$ across the shock at the terminal time $t = T$. This results in the adjoint solution having a uniform value along all characteristics leading backwards from the shock, as well as a constant value along each individual characteristic coming backwards in time from $t=T$.

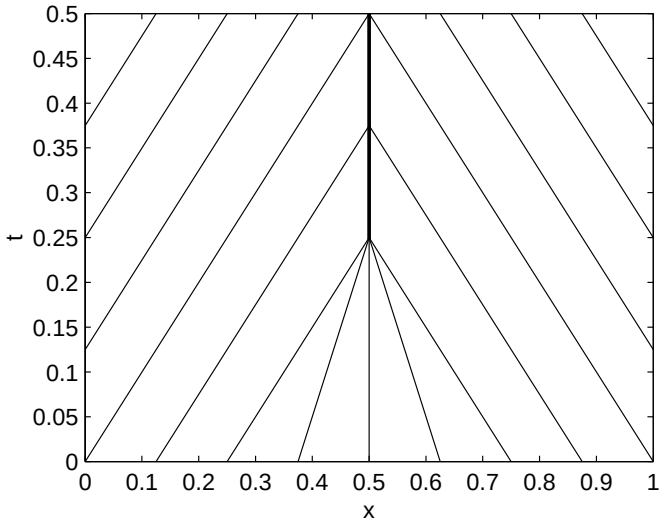


**Fig. 1.** Characteristics with a shock forming along $x = 0.5$.

## 3 Numerical discretisation

We consider a class of explicit finite volume discretisations of the form

$$\frac{1}{\Delta t} M \left( U^{n+1} - U^n \right) + \Delta F^n = 0.$$

Here $U^n$ is the vector of solution values $U_j^n, 0 \leq j \leq J$ at the $n^{th}$ timestep. $M$ is a diagonal mass matrix whose entries are

$$M_{jj} = \begin{cases} \frac{1}{2}(x_1 - x_0) & j = 0, \\ \frac{1}{2}(x_{j+1} - x_{j-1}) & 0 < j < J \\ \frac{1}{2}(x_J - x_{J-1}) & j = J, \end{cases}$$

Given a numerical flux $F_{j+1/2}$ which is a function of both $U_j$ and $U_{j+1}$, the flux difference $\Delta F^n$ is defined as

$$\Delta F_j^n = \begin{cases} F_{1/2}^n - f(u(0,t^n)) & j = 0, \\ F_{j+1/2}^n - F_{j-1/2}^n & 0 < j < J \\ f(u(1,t^n)) - F_{J-1/2}^n & j = J. \end{cases}$$

Note that this uses a weak implementation of the Dirichlet boundary conditions, as opposed to explicitly setting the values of $U_0^n$ and $U_J^n$. This weak treatment is preferable because it leads to a cleaner formulation of the adjoint discretisation.

Having computed the numerical solution, the discrete form of the nonlinear output functional is evaluated as

$$J = \sum_j M_{jj} G(U_j^N).$$

The linearised equations with the inclusion of the source term can be written as

$$\frac{1}{\Delta t} M \left( \tilde{U}^{n+1} - \tilde{U}^n \right) + A^n \, \tilde{U}^n = M \; S^n. \tag{3}$$

In addition, the linearised output functional is

$$\tilde{J} = g^T M \tilde{U}^N \equiv \sum_j \left( \frac{\mathrm{d}G}{\mathrm{d}u} \right)_j^N M_{jj} \tilde{U}_j^N.$$

In formulating the discrete adjoint equations, we follow what is often termed the "fully discrete" approach in which the goal is to define the adjoint equations in such a way as to obtain exactly the same value for the discrete linearised functional. This is in contrast to the "continuous adjoint" approach which directly discretises the adjoint differential equation, independently of the discretisation of the original nonlinear equation.

Considering to begin with the case in which $S^n = 0$ for $n > 0$, the linear discrete equations, (3), may be solved to obtain

$$\tilde{J} = \Delta t \; g^T M \left( I - \Delta t \, M^{-1} A^{N-1} \right) \ldots \left( I - \Delta t \, M^{-1} A^2 \right) \left( I - \Delta t \, M^{-1} A^1 \right) S^0.$$

This may be re-arranged as

$$\begin{aligned} \tilde{J} &= \Delta t \; g^T \left( I - \Delta t \, A^{N-1} M^{-1} \right) \ldots \left( I - \Delta t \, A^2 M^{-1} \right) \left( I - \Delta t \, A^1 M^{-1} \right) M S^0 \\ &= \Delta t \; (V^1)^T M S^0, \end{aligned}$$

where $V^1$ is obtained by solving the discrete adjoint equation

$$\frac{1}{\Delta t} \; M \left( V^{n+1} - V^n \right) + (A^n)^T \; V^{n+1} = 0, \tag{4}$$

subject to the final condition $V^N = g$.

Extending to the general case in which $S^n$ is non-zero at all time levels, the definition of the adjoint variables is unchanged and the resulting expression for the functional is

$$\tilde{J} = \Delta t \sum_{n=0}^{N-1} (V^{n+1})^T M S^n.$$

Note that this is a discrete equivalent of equation (2).

We will continue to use the same adjoint discretisation when the flow solution contains a shock. The question to be investigated is whether this will automatically capture the correct adjoint solution in the limit of increasing grid resolution. As a prelude, we note that only $g \equiv \mathrm{d}G/\mathrm{d}u$ enters into the adjoint calculation as initial data, not $[G]$ and so it is not clear that the adjoint calculation has the information necessary to correctly predict the adjoint solution in the neighbourhood of the shock.

## 4 Numerical tests

The numerical tests are all performed with the Burgers equation, $f(u) \equiv \frac{1}{2}u^2$, with initial conditions

$$u(x,0) = \begin{cases} 1, & x < 0.25 \\ 2 - 4x, & 0.25 \le x \le 0.75 \\ -1, & x > 0.75 \end{cases}$$

and boundary conditions $u(0,t) = 1,\ u(1,t) = -1$. As shown in Figure 1, a stationary shock forms at $x = 0.5$ at time $t = 0.25$.

To assess the degree to which the solutions are grid converged, numerical results are obtained on two uniform grids with $\Delta x = 0.0025, 0.005$. The corresponding timesteps are $\Delta t = 0.4\Delta x$ giving a maximum CFL number of 0.4.

The output functional uses $G(u) = u^5 - u$. This gives $g(x) = 4$ on either side of the shock. Furthermore, the jump $[G]$ across the shock is equal to zero, so the analytic solution has $v = 0$ for all backward travelling characteristics emanating from the shock. Hence the complete adjoint solution is

$$v(x,t) = \begin{cases} 4, & x < t \\ 0, & t < x < 1 - t \\ 4, & x > 1 - t \end{cases}$$

### 4.1 Riemann flux

The first results use a first order Riemann numerical flux function,

$$F(u_1, u_2) = \frac{1}{2} \max\left( \left(\max(0, u_1)\right)^2, \left(\min(0, u_2)\right)^2 \right).$$

The upper two plots in Figure 2 show the nonlinear and adjoint solution at times $t = 0.1, 0.4$. There is very little difference between the solutions for the two grids. However it is very clear that the adjoint solution is completely wrong in the region emanating from the shock, where the computed value is approximately equal to $-1$.

The cause for this incorrect value can be seen in the lower two plots which show the nonlinear and adjoint solutions at the final time $t = 0.5$, plotted versus node number relative to the central node at $x = 0.5$. It is seen that on both grids the nonlinear solution has a single shock point at which $u = 0$. For this point the corresponding adjoint value is $g = \mathrm{d}G/\mathrm{d}u(0) = -1$, and a detailed examination of the matrix $A$ reveals that this value is propagated backward in time along the length of the shock, and along any characteristic which propagates out of the shock.

An even more dramatic example of incorrect behaviour would be obtained by using an odd number of cells instead of an even number, so that the shock

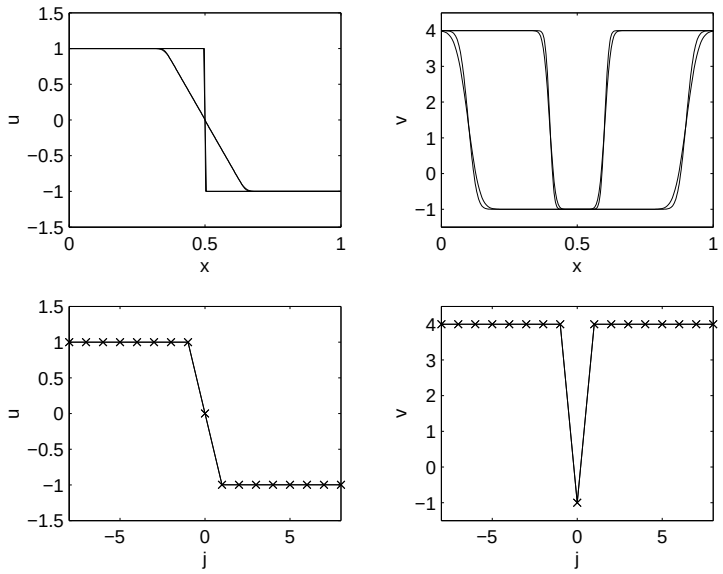


**Fig. 2.** Nonlinear and adjoint solutions obtained with the Riemann flux function, for $t=0.1, 0.4$ in the upper plots, and $t=0.5$ in the lower plots.

centre lies half-way between two nodes. In that case, the final solution would have no interior shock point, and so all of the elements of $g$ would have the value 4, leading to the entire discrete adjoint solution having value 4.

### 4.2 Lax-Friedrichs flux

The rest of the results all use a simple Lax-Friedrichs flux, combining a central average flux with additional first order smoothing,

$$F(u_1, u_2) = \frac{1}{2}\left(f(u_2)+f(u_1)\right) - \mu\,(u_2-u_1)\,.$$

Figure 3 shows results for $\mu=0.25$. The values computed on the two grids are almost identical. In the vicinity of the shock, the nonlinear solution is very close to a self-similar steady-state solution which depends solely on $\mu$ and the grid ratio $\Delta t/\Delta x$, and with this level of smoothing there is again only one grid point in the middle of the shock. The adjoint solution appears grid converged, but to a value which is incorrect.

Figure 4 shows results for $\mu=1.0$. There are now many grid points across the shock, and therefore fairly good resolution of the differing values of $g = \mathrm{d}G/\mathrm{d}u$ for $u$ ranging from 1 on the left of the shock to $-1$ on the right of the shock. The numerical adjoint solution now has a value very close to the analytic value of zero in the central part of the domain.

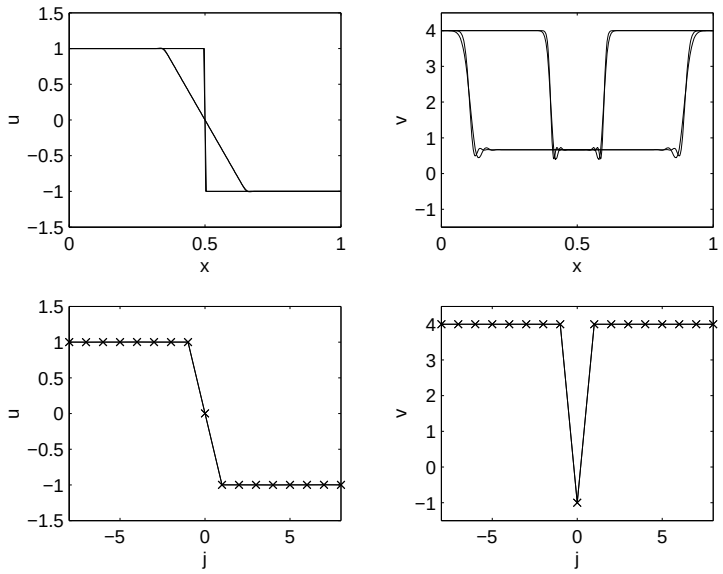


**Fig. 3.** Nonlinear and adjoint solutions obtained with the Lax-Friedrichs flux with smoothing $\mu = 0.25$, for $t = 0.1, 0.4$ in the upper plots, and $t = 0.5$ in the lower plots.

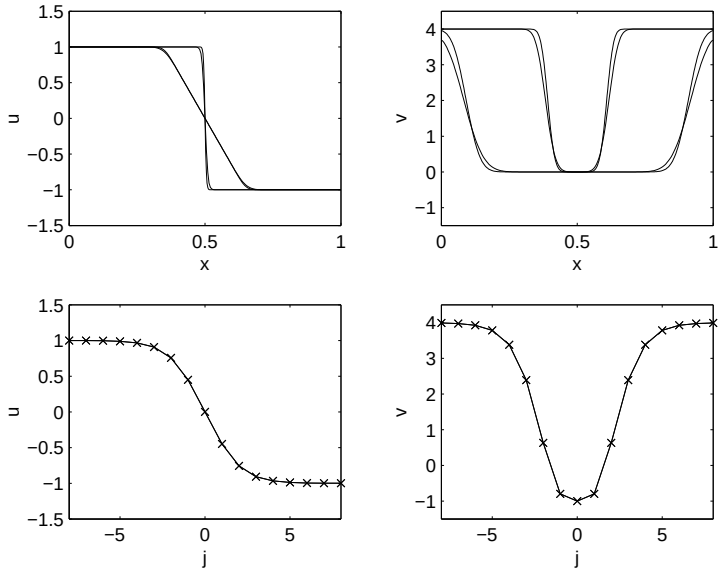


**Fig. 4.** Nonlinear and adjoint solutions obtained with the Lax-Friedrichs flux with smoothing $\mu = 1.0$, for $t = 0.1, 0.4$ in the upper plots, and $t = 0.5$ in the lower plots.

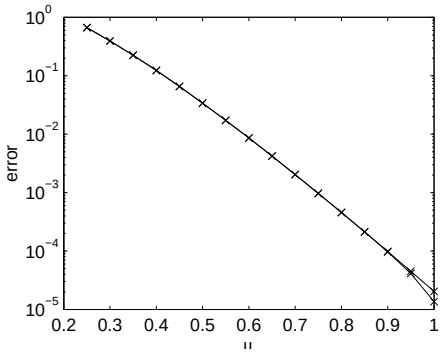


**Fig. 5.** Error in the computed value for $v(0.5, 0)$ as a function of the numerical smoothing coefficient $\mu$.

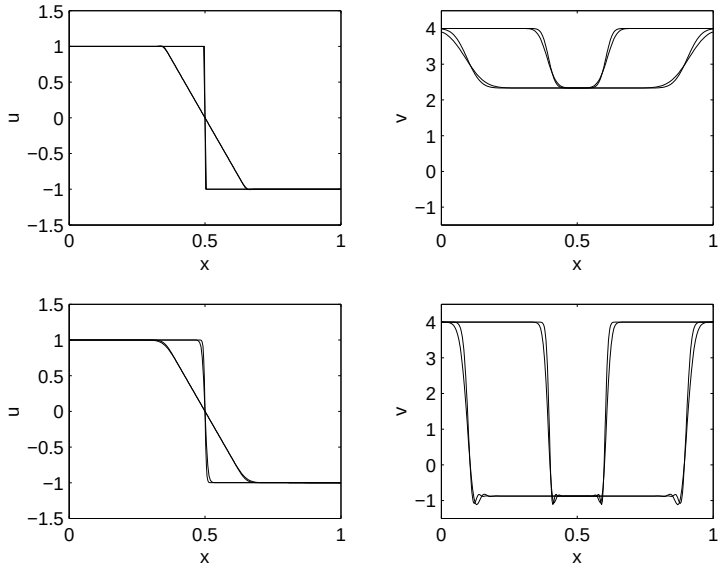


**Fig. 6.** Solutions at $t = 0.1, 0.4$ obtained with the Lax-Friedrichs flux with different levels of smoothing in the nonlinear and adjoint calculations. Upper results: $\mu$(nonlinear) $= 0.25$, $\mu$(adjoint) $= 1.0$. Lower results: $\mu$(nonlinear) $= 1.0$,, $\mu$(adjoint) $= 0.25$.

Figure 5 plots the error in the computed value for $v(0.5, 0)$ versus the value of the smoothing coefficient $\mu$. It appears from these results that the error decreases exponentially with the value of $\mu$ and hence the number of grid points across the shock.

Figure 6 presents results obtained by using different values for $\mu$ in the nonlinear and adjoint calculations. The upper results use $\mu = 0.25$ for the nonlinear calculations, and $\mu = 1.0$ for the adjoint calculation. The higher

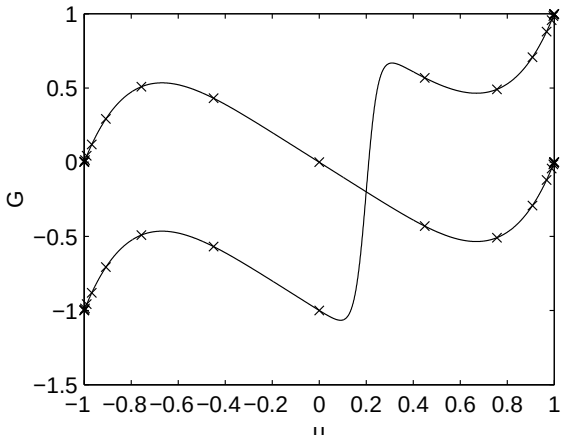


**Fig. 7.** Two objective functions $G(u)$.

value for $\mu$ in the adjoint calculation leads to rapid diffusion bringing into the shock region the larger values for the adjoint solution $v(x,t)$ on either side of the shock, leading to incorrect values in the shock region. The lower results use $\mu = 1.0$ for the nonlinear calculations, and $\mu = 0.25$ for the adjoint calculation. The lower value for $\mu$ in the adjoint calculation leads to very little diffusion, and so the adjoint solution value $g = -1$ at the centre of the smeared shock is convected backwards in time leading to $v(x,t) \approx -1$ throughout the shock region. These results show the importance of using the same value of $\mu$ in both calculations, so that the adjoint discretisation corresponds correctly to the linearisation of the nonlinear discretisation.

## 5 Discussion

One clear conclusion from these numerical results is that there must be consistency between the nonlinear and adjoint calculations regarding the level of numerical smoothing. Also, for convergence it is necessary that as the grid resolution improves, the numerical smoothing varies in a way which increases the number of points across the shock, while at the same time the overall width of the shock decreases.

To understand why this latter point is fundamental, and not just a feature of the particular numerical experiments conducted, we need to consider the information supplied to the adjoint code. The analytic solution has a value along the shock which depends on the jump $[G(u)]$ across the shock at the final time $t = T$. However, the end conditions for the numerical adjoint solution are given by the values of $\mathrm{d}G/\mathrm{d}u$ for the final values of $u$ obtained from the nonlinear calculation. These means that the numerical solution must implicitly evaluate $[G(u)]$ by some process which effectively integrates $\mathrm{d}G/\mathrm{d}u$

across the smeared shock. For this to be done accurately requires adequate resolution of the variation in $\mathrm{d}G/\mathrm{d}u$.

This point is illustrated in Figure 7. The smoother of the two curves is $G(u)=u^5-u$, the objective function in the numerical experiments. The symbols correspond to the values of $u$ at the final time $t=T$ in Figure 4. The second curve is $G(u) = u^5-u+\tanh 20(u-0.2)$. This function has almost identical gradient values at the indicated sampling points, and therefore produces a numerical adjoint solution which is visually indistinguishable from Figure 4. However, the analytic solution has a different jump in $G(u)$ across the shock, and so the analytic solution is quite different. This shows that for any numerical discretisation with a fixed number of points across the shock, it is easy to construct an objective function for which the numerical adjoint solution will not converge.

## References


[BJ98] F. Bouchut and F. James. One-dimensional transport equations with discontinuous coefficients. *Nonlinear Analysis*, 32:891–933, 1998.

[BR01] R. Becker and R. Rannacher. An optimal control approach to error control and mesh adaptation. In A. Iserles, editor, *Acta Numerica 2001*. Cambridge University Press, 2001.

[Gil02] M.B. Giles. Adjoint equations and discrete approximations in the presence of shocks. Technical Report NA02/10, Oxford University Computing Laboratory, 2002.

[GP98] M.B. Giles and N.A. Pierce. On the properties of solutions of the adjoint Euler equations. In M. Baines, editor, *Numerical Methods for Fluid Dynamics VI*. ICFD, Jun 1998.

[GP01] M.B. Giles and N.A. Pierce. Analytic adjoint solutions for the quasi-one-dimensional Euler equations. *J. Fluid Mech.*, 426:327–345, 2001.

[HCL94] K.C. Hall, W.S. Clark, and C.B. Lorence. A linearized Euler analysis of unsteady transonic flows in turbomachinery. *J. Turbomachinery*, 116:477–488, 1994.

[Jam95] A. Jameson. Optimum aerodynamic design using control theory. In M. Hafez and K. Oshima, editors, *Computational Fluid Dynamics Review 1995*, pages 495–528. John Wiley & Sons, 1995.

[LG94] D.R. Lindquist and M.B. Giles. Validity of linearized unsteady Euler equations with shock capturing. *AIAA J.*, 32(1):46, 1994.

[PG00] N.A. Pierce and M.B. Giles. Adjoint recovery of superconvergent functionals from PDE approximations. *SIAM Rev.*, 42(2):247–264, 2000.

[Tad91] E. Tadmor. Local error estimates for discontinuous solutions of nonlinear hyperbolic equations. *SIAM J. Numer. Anal.*, 28:891–906, 1991.

[Ulb02a] S. Ulbrich. Adjoint-based derivative computations for the optimal control of discontinuous solutions of hyperbolic conservation laws. *Systems & Control Letters*, to appear, 2002.

[Ulb02b] S. Ulbrich. A sensitivity and adjoint calculus for discontinuous solutions of hyperbolic conservation laws with source terms. *SIAM J. Control and Optim.*, to appear, 2002.